Studies on Coil-less Reluctance Force Actuators

Marcus Herrmann and Heinz Ulbrich
Institute of Applied Mechanics – Technical University Munich
85748 Garching, Boltzmannstr. 15
{herrmann, ulbrich}@amm.mw.tum.de

***Abstract*— Flux control in magnetic actuators can be achieved by additional field superposition or flux path manipulation. Usually, coils are used for external flux control, but inductance lags and ohmic losses degrade actuator efficiency. To design energy-efficient reluctance force actuators innovative concepts for controlling the magnetic flux without coils are investigated. On the one hand, this contribution deals with variable reluctance elements based on the inverse magnetostrictive effect. On the other, magnetic flux is redirected in the magnetic circuit by means of small displacements of reluctance switch elements. For high manipulation rates these elements feature cog-slot structures. Some general design rules are outlined and two examples of application are presented. An active magnetic bearing and a bidirectional actuator are simulated and compared to a bipolar electromagnetic actuator. Finally, all results show the capability of coil-less reluctance force actuators to outperform present electromagnetic systems in terms of bandwidth and energy balance.**

***Index Terms*— reluctance switch, permanent magnet, flux path control, actuator control**

I. Introduction

The reluctance force principle owns a high force-volume ratio and allows the design of compact energy-efficient actuators. Because of their high force density reluctance forces are utilised in high performance magnetic bearings or in levitation actuators. Reluctance forces are characterised primarily by the flux $\Phi = B \cdot A$ through a permeability interface and its cross-sectional area A as (1) indicates for a homogeneous magnetic flux density B normal through an iron-air interface:

$$F = \frac{B^2 A}{2\mu_0} = \frac{\Phi^2}{2\mu_0 A}. \tag{1}$$

Coils are very convenient for controllability of flux by superposition of the main flux with another flux. Still, a major disadvantage is Joule loss in the windings reducing efficiency and deteriorating material properties. Moreover, coil resistance-inductance form a low-pass system limiting actuator bandwidth. Bipolar actuators featuring coils and bias permanent magnets achieve a better energy balance by avoiding static operation currents almost completely. To completely discard any heat loss in magnetic actuators coils must vanish, which necessitates alternatives for magnetic flux control.

In this paper methods of flux control without coils are investigated. Defined variations of the magnetic reluctance in certain parts of the magnetic circuit are the key for flux control. If a magnetic system can be modelled with lumped parameters (equivalent magnetic network), then the magnetic reluctance R_{mag} of a path element is defined by (2) with length l, cross-sectional area A and magnetic permeability $\mu = \mu_0 \mu_r$

$$R_{mag} = \frac{l}{\mu A}. \tag{2}$$

First, smart material based reluctance variations due to changing permeability μ are investigated. Experiments with magnetostrictive amorphous ribbons validate the force manipulation. In the second part, a reluctance switch with varying cross-sectional area A is proposed. Using cog-slot structures, an efficient reluctance variation during small deviations of the switch element is achieved. Calculations and design rules are applied to examples for actuator and magnetic bearing, which show a high force variation and perfect energy balance. Finally, results are compared to given electromagnetic actuator and control strategies are derived to exploit the improved dynamic capabilities of coil-less reluctance force actuators.

II. Variable Reluctance Elements

A. High Reluctance Elements (HRE)

Variation of path reluctance can be achieved by smart materials altering their reluctance depending on external conditions. Giant magnetostrictive materials (GMM) form such a class, which is investigated thoroughly by [1]–[3]. They use a composite of piezoelectric actuator and GMM (Terfenol-D) to form a high reluctance element R_{Mp} with a low relative permeability range $\mu_r = 3 \ldots 10$, which is placed parallel to the working air gap R_G (Fig. 1a). To achieve an even higher force drop a reluctance R_{Ms} is placed serially to the working air gap (Fig. 1b) and mutual inverse variation of R_{Mp} and R_{Ms} is proposed. Evaluation of the equivalent magnetic network in Fig. 1b)

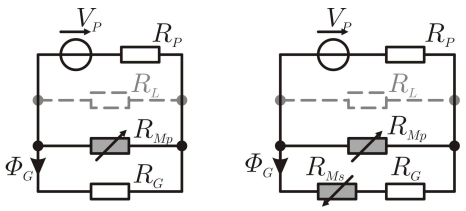

a) parallel only b) parallel & seriell

Fig. 1. HRE configuration in equivalent magnetic network

with (3) based on data from [2] reveals a greater force drop on the air gap during the permeability change in the variable reluctance elements (Fig. 2a).

$$F_G = \frac{V_P}{\mu_0 A \left[\frac{R_P}{1-\sigma_L}\left(1+\frac{R_G+R_{Ms}}{R_{Mp}}\right)+R_G+R_{Ms}\right]^2} \quad (3)$$

The results obtained are based on a magnetic circuit with constant cross-sectional area and NdFeB permanent magnet source ($_BH_C = 1000$ kA·m^{-1}, $B_r = 1.2$ T, $\sigma_L = 25$ % leakage). The improved force manipulation becomes more obvious with two single actuators operating in difference configuration. They form a simple magnetic bearing exhibiting a 18 % higher overall force change compared to an actuator with parallel reluctance elements only (Fig. 2b).

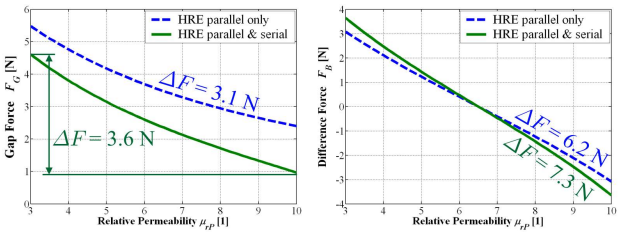

a) Single actuator b) Difference configuration

Fig. 2. Force variation for different HRE configurations

B. Low Reluctance Elements (LRE)

As (3) reveals, the lower the reluctance of serial elements R_{Ms} the better force manipulation. Based on the inverse magnetostrictive effect, amorphous alloys are low reluctance elements (LRE), which offer a high mechanical induced change of susceptibility, low saturation magnetostriction λ_S and high mechanical stress capacity [4]. A special type are nanocrystalline soft magnetic alloys with positive or even negative magnetostriction. Relative permeability of such materials depends amongst other on mechanical stress σ:

$$\mu_r = \frac{J_S^2}{2\mu_0 K} \quad (4)$$

with saturation magnitisation J_S and induced anisotropy energy constant K

$$K = K_0 - \frac{3}{2}\lambda_S \cdot \sigma \quad (5)$$

Good soft magnetic alloys have a low magnetic anisotropy, which infers a low coercitivity and high permeability [5]. Experiments with low reluctance elements used nanocrystalline VITROVAC ribbons (VAC Vacuumschmelze Hanau GmbH: $J_S = 0.86$ T, $K_0 = 206.4$ J·m^{-3}, $\lambda_S = 11$ ppm, $t = 25\,\mu$m). Clearly, mechanical stress is limited regarding to (5) to $\sigma_{max} = {}^{2K_0}/_{3\lambda_S} = 12.5$ N·mm^{-2}, otherwise the induced anisotropy will be destroyed. With a stress variation $\sigma = 0 \ldots 11.5$ N·mm^{-2} relative permeability

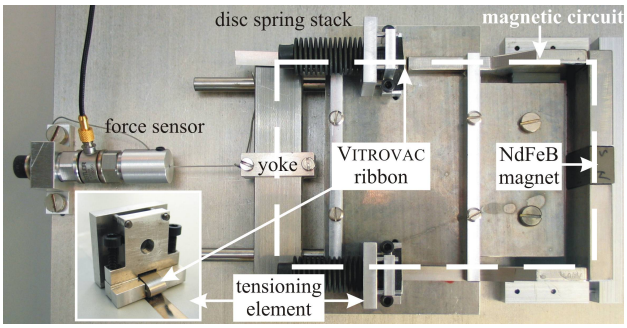

Fig. 3. Experiment setup for flux manipulation with LRE

changes between $\mu_r = 1426 \ldots 17674$ by a factor of 12.4, which is four times the factor of Terfenol-D ($\mu_r = 3 \ldots 10 \rightarrow 3.3$).

A basic experiment for flux manipulation with LRE was conducted using the VITROVAC ribbons being wound on a core of a tensioning element to vary mechanical stress in the ribbon. The serial magnetic circuit with two tensioning elements, permanent magnet, soft iron core and guided movable yoke is shown in Fig. 3. Pull-off force of the yoke from the iron core was measured repeatedly on stress-free ribbons as well as under mechanical load. The experimental results in Fig. 4 show more than 10 % force variation in both ways. They also confirm the nanocrystalline property of increasing permeability with rising magnetostriction due to mechanical stress. With their high permeability such amorphous materials may be an alternative for serial elements in a magnetic circuit as proposed in Fig. 1b).

Yet, some inherent properties may limit actuator application of amorphous materials. First, usually they are manufactured as thin ribbons ($t \leq 25\,\mu$m) complicating creation of required cross-sectional area. Second, mechanical stress must be applied uniformly to all ribbons. Third, in contrast to sensor systems [6] actuation systems are efficient only, when the reluctance of variable elements R_M and air gap R_G equal. Finally, all magnetostrictive materials posses hysteretic behaviour, which might be deteriorated by likewise hysteretic piezoelectric actuators [3]. Nevertheless, high performance actuators with high bandwidth should avoid such drawbacks from the start.

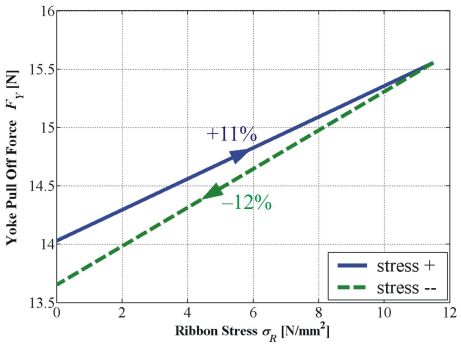

Fig. 4. Measured pull off force related to stress in nanocrystalline ribbon

III. Reluctance Switch Elements

A. Classification and Previous Research

The principle of magnetic flux control is a key for magnetic actuator performance (Fig. 5). Equation (2) reveals a reluctance dependency on permeability μ (Sec. II), element length l and cross-sectional area A. Reference [7] proposed a magnetic suspension system with a linear actuator, which varies air gap length l to balance a ferromagnetic object in equilibrium levitation position. Because of $R_{mag} \sim l$ achievable reluctance variations are small and restricted to low frequencies. Another innovative option for flux control is a variation of its path (Fig. 5 bottom rightmost).

Control of air gap forces by flux redirection can be achieved by lowering the desired path reluctance whereas any other path reluctance should increase. Fig. 6a) shows the basic design of such a *magnetic reluctance switch*, which usually requires a bypass path. Reference [8] investigated a flux path control magnetic suspension using a variable overlap of permanent magnet and ferromagnetic plates. A kind of reluctance switch was used, but a significant change in reluctance still demanded a rather large area travel. In order to have a high response system, already small area changes should bring about high effects. Thus, all flux switching presented in this paper will be based on changes of cross-sectional area A effecting reluctance R_{mag} quickly because of the inverse law (2).

B. Principle and Calculation

High response coil-less actuator necessitate little switch travel. Small switch pole areas favour short switching times but also undesired saturation effects. A new approach for a reluctance switch is based on variable reluctance stepping motors, which minimise consecutively the reluctance of energised phases to align the many stator and armature poles for traveller motion [9]. The reversal of this principle involves a magnetic flux dependence on the displacement between opposing poles influencing air gap reluctance significantly, mostly because of effective pole area overlap. Thus, variable reluctance elements can be formed by using two opposing arrays of poles, each resembling a cog-slot structure. In [10] an axial magnetic bearing using a similar teeth contour was presented to centre its rotor axially.

An accurate calculation of fields and forces in magnetic actuators requires convenient modelling to reproduce all important aspects. The proposed cog-slot-structures

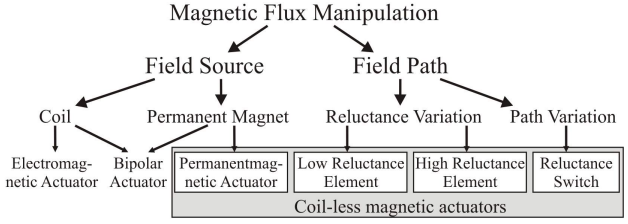

Fig. 5. Options for flux manipulation in magnetic actuators

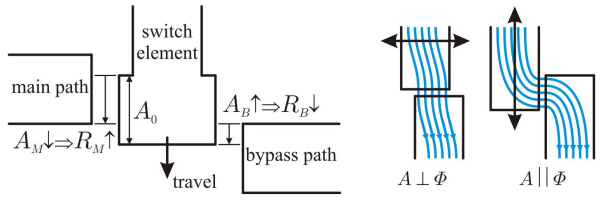

a) Basic Reluctance Switch b) Area - Flux Alignment

Fig. 6. Reluctance switch based on cross-section area change

are highly complex geometries with a number of free design parameters (Subsec. III-C). Equivalent magnetic networks may be a rough method for field estimation in simple structures, when flux distribution is homogeneous. This holds as long as the pole areas have small normal distance, are perpendicular to the magnetic flux direction and their tangential displacement is less than the pole width. However, small cog-slot structures usually exhibit a nonlinear behaviour, i.e. immense fringing effects, cogging forces and saturation. For reliable reluctance switch design, the finite element method (FEM) with ANSYS is used, where nonlinear material properties and complex geometries can be precisely evaluated.

C. Design of Reluctance Switch Elements

For reluctance switch design the cross-sectional area A is important, which may be perpendicular or parallel to the primary magnetic flux direction (Fig. 6b). FEM calculations revealed a superior flux control with parallel area configuration compared to the perpendicular one. In the parallel arrangement a switch with n_S teeth has $2n_S$ cross-sectional areas (i.e. reluctance elements), whereas a perpendicular system has only n_S areas to be varied. In Fig. 7a) major design parameters are pictured: cog number n_S, cog width b_C, cog height h_C, nominal switch travel s_0, lateral gap t_L and initial overlap t_0 of opposing pole cogs.

For high response actuation nominal switch travel s_0 should be preferably small ($s_0 \leq 1$ mm). High flux switching rates were observed on structures having a cog height $h_C \approx 1$ mm. Then cross-sectional areas change rapidly, but fringing effects on cogs occur. Optimal design also involves a nominal switch reluctance tuned to the reluctance of main and bypass flux path, whose cogs may have different geometry. Calculations revealed, that particularly the initial overlap t_0 of opposing poles is

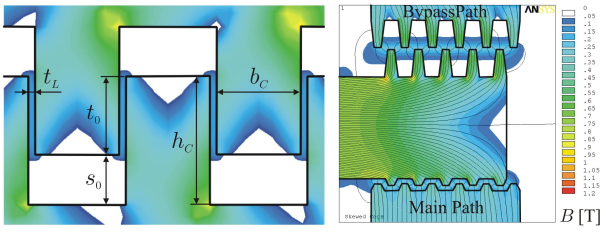

a) Cog Parameters b) Skewed Cogs

Fig. 7. Design of parallel reluctance switch elements

important for reluctance adjustment. Main path cogs having a height $h_{Cm} \approx s_0$ should not overlap initially ($t_0 < 0$) for efficient switch operation, whereas bypass path cogs may be higher ($h_{Cb} > 1.5 \cdot s_0$) and should overlap with $t_0 \approx {}^{h_{Cb}}/_{10} > 0$.

In a magnetic circuit all flux should pass through identical cross-sectional areas. Thus, a high number of cogs with small width seems preferable in terms of switch travel. However, manufacturing will limit minimal cog width and thus cog number. Lateral cog gap t_L should be chosen as small as possible depending on manufacturing processes. In simulations, a main path geometry ratio ${}^{b_{Cm}}/_{h_{Cm}} \approx 1$ and a lateral gap $t_L < {}^{b_C}/_2$ showed satisfying results.

One major problem in all systems using cogs is cogging force. This unsteady backward force will be challenging for precise switch positioning and demand special actuators. However, a variety of research dealt with modelling and minimisation of this disturbing phenomenon [11]–[14]. Besides pole shifting and special design rules the use of skewed cogs is mandatory (Fig. 7b), allowing a smooth change of reluctance during switch motion.

D. Application Examples

The proposed reluctance switch elements were implemented in typical magnetic systems to confirm their utilisability. First, the active magnetic bearing (AMB) element in Fig. 8 with permanent magnet source was simulated (object depth: 100 mm), where four such elements would form a radial AMB. Primary design objectives were maximum variation of rotor attraction force (Fig. 9a) as well as a minimum variation of switch deflection force (Fig. 9b) during switch travel. The AMB element has main path cogs being offset by $t_0 = -0.5$ mm whereas the bypass cogs have $t_0 = +0.5$ mm overlap. Calculation results in Fig. 9a) show a 60 % higher rotor attraction force variation over switch travel with skewed cogs (solid line) compared to rectangular ones (dashed line). Even more important the switch deflection force in Fig. 9b) remains almost constant due to smooth reluctance change. A compensation of the switch deflection force

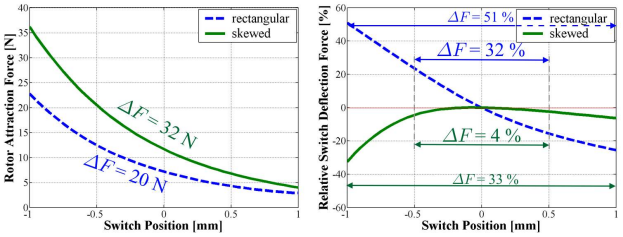

a) Rotor attraction force b) Switch deflection force (normalised)

Fig. 9. Forces in AMB element with rectangular and skewed cogs

in initial switch position with springs would enable rotor force control by an almost vanishing actuation force. Here, for a switch deflection of ± 0.5 mm only 2.5 N actuation force (4 %) are required to change rotor attraction force between $(6.8 \ldots 20.5)$ N, which gives a superior effect-actuation force ratio of 5.5.

The second application example in Fig. 10 is related to a formerly presented bidirectional electromagnetic actuator with double pull-disc armature [15]. Whilst in AMBs the air gap is usually small and nearly constant, this actuator features a 2 mm armature stroke. For flux manipulation, the reluctance switch is able to rotate with tiny deflections of ± 1.25 degrees. Moreover, the reluctance switch has serial (left end) and parallel (right end) elements for a high flux switching capability. Instead of a bypass path there are two main circuits through the pull discs to whom the flux is switched for bidirectional operation. All cogs are 1 mm high, skewed by 45 degrees and opposing cogs are offset by $t_0 = -0.5$ mm.

FEM calculations focussed on armature actuation force and switch deflection force, each dependent on armature position and switch deflection. Fig. 11A) holds pure magnetic forces showing very smooth force variations with almost constant slopes. Thus, the armature experiences an average magnetic stiffness $c_{MA} = -155$ N·mm^{-1} (model depth: 100 mm). Applying a stiffness compensation with a spring $c_{FA} = -c_{MA}$ gives an actuation force nearly independent from armature position (Fig. 11b.1), which can be controlled almost linearly by switch position. The switch also is subject to a negative magnetic torsional stiffness $c_{MS} = -3.5$ Nm·deg^{-1}, which may be compensated by

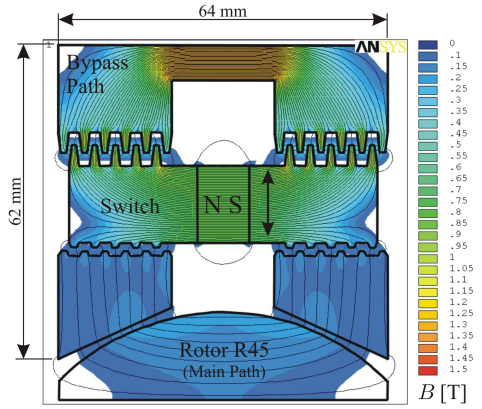

Fig. 8. AMB element with skewed cogs, bypass path and quarter rotor

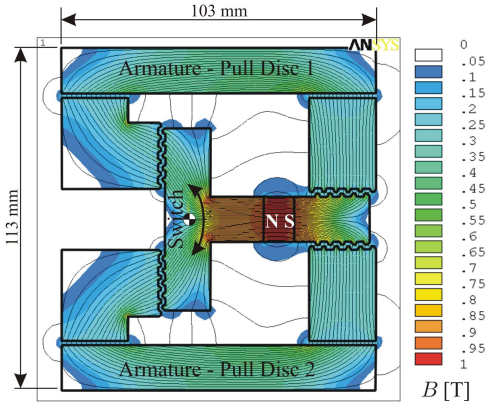

Fig. 10. Actuator design with skewed cogs and double pull-disc armature

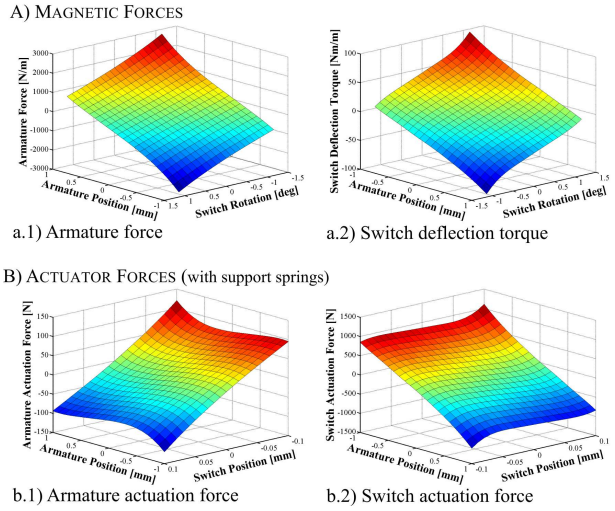

Fig. 11. Forces of bidirectional actuator in Fig. 10

an axial spring $c_{FS} = -\frac{c_{MS}}{l_F^2 \sin(1°)} = 495$ N·mm^{-1} placed $l_F = 20$ mm from the axis of rotation. Fig. 11b.2) shows the switch deflection force which another actuator has to exert on a 5 mm lever after stiffness compensation. To sum up, force on the switch is independent from switch position and varies only with armature position.

Finally, the presented actuator can be considered as a mechanical transformer using higher forces with very low stroke (± 1 kN $\times$ ± 0.1 mm = 100 N·mm) to achieve considerable forces on a larger stroke (± 100 N $\times$ ± 1 mm = 100 N·mm), i.e. input energy equals output energy. The switch needs 1 kN actuation force on 0.1 mm stroke only, which refers directly to high response piezoelectric devices to ensure a high bandwidth of the actuation system in Fig. 10. To conclude, this actuator has a perfect energy balance with 100 % efficiency, i.e. no transformation losses and it has the potential for high operation bandwidth.

IV. Control of Reluctance Force Actuators

A. Bipolar Electromagnetic Linear Actuator

In Reference [15] the electromagnetic actuator in Fig. 12 with two pull-discs for ± 2.5 mm bidirectional stroke is investigated in terms of systematic control. The built-in bias NdFeB permanent magnets guarantee high forces at low power consumption, but they introduce a

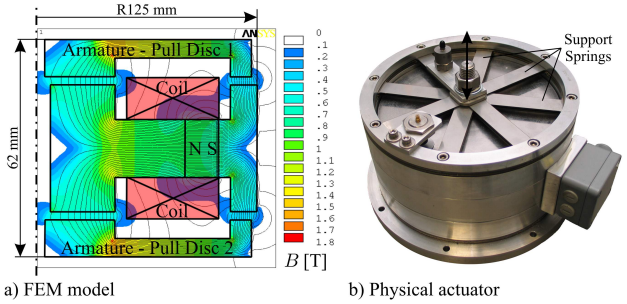

Fig. 12. Electromagnetic actuator with double pull-disc armature

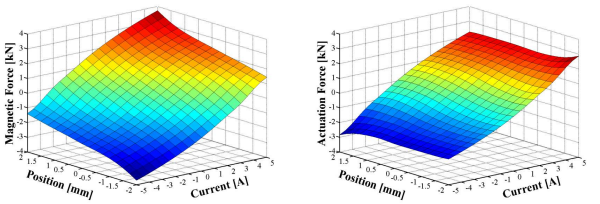

Fig. 13. Armature forces of electromagnetic actuator in Fig. 12

negative magnetic stiffness being plotted in Fig. 13a). The actuator armature is supported radially stiff by leaf springs, which reduce negative stiffness in axial direction (Fig. 13b). The comparison of Fig. 13b) with Fig. 11b.1) reveals a strong analogy in actuation force characteristic of electromagnetic and coil-less system. In both cases an almost position independent armature force is achieved by means of springs.

B. System Components and Controller Structure

A magnetic actuator can be structured into three basic system components depicted in Fig. 14, each having characteristic transfer behaviour. Both reluctance switch version and electromagnetic system feature equivalent second order mechanical systems as well as identical magnetic systems governed by hysteresis and eddy currents, which may be approximated by a first order lag. Major differences concern the power supply subsystem, which in the electromagnetic case includes voltage amplifier and coil, creating a resistance-inductance circuit. In fact, variations of current i and armature position q alter the inductance L, but a first order lag approximation proved useful. In contrast, power supply subsystem for the reluctance switch actuator in Fig. 10 comprises transfer behaviour from switch deflection force to its position. The mechanical system of switch mass and stiffness compensation spring is second order. For generation of adequate forces along a tiny stroke (± 1 kN $\times$ ± 0.1 mm) piezoelectric actuators are proposed. Approximating the piezoelectric actuators as second order system finally results in a fourth order power system. However, the cut-off frequencies of piezoelectric systems are usually in the kHz-range. Moreover, a high switch compensation stiffness $c_{FS} = 495$ N·mm^{-1} on a quite small switch mass $m_S \approx 0.5$ kg gives a resonance frequency of 160 Hz, which is much higher than the corner frequency $f_{RL} = 10$ Hz of the actual RL-circuit ($R = 11\ \Omega$, $L = 180$ mH).

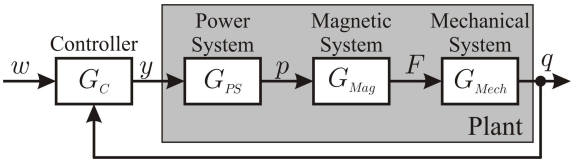

Fig. 14. Main components of magnetic actuation systems

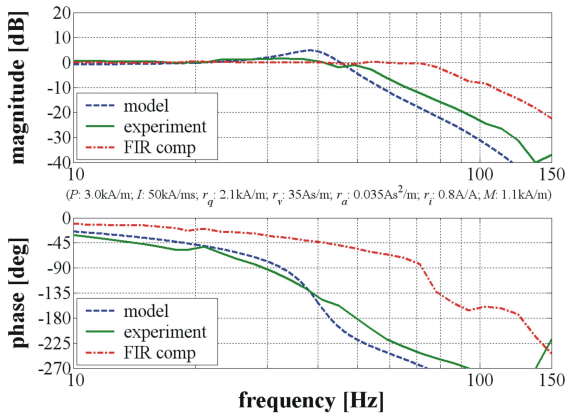

Fig. 15. Bode plot of PI state feedback control with feedforward element including model behaviour, experiment result without and with forward FIR compensation [15]

For convenient control of the unstable, undamped bipolar electromagnetic actuator a state space controller with a PI feedback path was implemented. Transfer behaviour with a load $m = 35$ kg in Fig. 15 is good-natured for model (dashed) and experiment (solid). The original bandwidth of circa 50 Hz can be increased significantly by a series forward compensation with a controller outside the feedback loop not affecting the poles of the original control system. In this case, measured transfer function data is inverted for usage in a Finite Impulse Response (FIR) filter, which achieves an impressive 80 Hz bandwidth limited by the supply voltage of 200 V only (dash-dot line).

Turning to the coil-less actuator, similar state space models and control methods can be used, because piezoelectric actuators are widely used and thoroughly investigated. Moreover, the power subsystem may even feature linear behaviour in a range where inductance limits bandwidth in electromagnetic drives already. For that reasons, the authors are certain about superior dynamic capabilities of reluctance switches actuators.

V. Conclusion

This contribution presented studies on magnetic coil-less reluctance force actuators, which avoid heat and improve bandwidth. Basically, there are two options for coil-less flux manipulation, i.e. to change flux path reluctance or to change the flux path itself. Investigations started with variable reluctance elements using the inverse magnetostrictive effect and lumped network analysis for optimal element placement. A combination of high reluctance elements parallel to the working air gap and low reluctance elements in series to the air gap showed an improved force manipulation characteristic. Moreover, all magnetic reluctance elements should be tuned to the governing air gap reluctance in the magnetic circuit. Reluctance switch elements promised better capabilities for flux control transferring the magnetic flux between desired destinations. The proposed reluctance switches have a cog-slot structure similar to stepper motors. Positioning and design of such reluctance switch elements were investigated for high actuator performance, where skewed cogs and parallel configurations proved inevitable. Some design rules were outlined and two typical examples of application using high energy permanent magnets only were simulated, which show high magnetic forces on a compact design. Moreover, actuator force manipulation was energy neutral with a 100 % efficiency. Finally, state space control for reluctance actuators was presented based on experience with an electromagnetic system asserting an improved bandwidth for coil-less reluctance force actuators.

References

[1] T. Ueno, J. Qiu, and J. Tani, "Magnetic force control based on the inverse magnetostrictive effect," *IEEE Transactions on Magnetics*, vol. 40, pp. 1601–1605, May 2004.

[2] T. Ueno and T. Higuchi, "Dynamic response in magnetic force control using a laminate composite of magnetostrictive and piezoelectric materials," *IEEE Transactions on Magnetics*, vol. 41, pp. 1082–1085, March 2005.

[3] T. Ueno and T. Higuchi, "Novel composite of magnetostrictive material and piezoelectric actuator for coil-free magnetic force control," *Sensors and Actuators A*, vol. 129, pp. 251–255, May 2006.

[4] D.-J. Jendritza, ed., *Technischer Einsatz Neuer Aktoren*. Renningen-Malmsheim: expert (Kontakt & Studium, Bd. 484), 1995.

[5] G. Herzer, *Handbook of Magnetic Materials, Chapter 3: Nanocrystalline soft magnetic alloys*, vol. 10. Elsevier Science B.V., 1997.

[6] J. Seekircher, *Magnetoelastische Kraftsensoren mit amorphen Metallen*. No. 266 in Fortschr.-Ber. VDI Reihe 8, Duesseldorf: VDI Verlag, 1991.

[7] K. Oka, M. Hasegawa, T. Morita, and T. Higuchi, "Study of 2dof magnetically suspended manipulation system with air gap control," in *The 7th International Symposium on Magnetic Bearings*, pp. 251–256, August 2000.

[8] T. Mizuno, H. Hoshino, M. Takasaki, and Y. Ishino, "Flux path control magnetic suspension," in *The 9th International Symposium on Magnetic Bearings*, pp. 549–554, August 2004.

[9] H. Gatzen, H.-D. Stoelting, and B. Ponick, "Alternatives for micromachined linear actuators," in *Actuator 2004*, pp. 317–320, June 2004.

[10] W. Lee, W. Canders, and W. Schumacher, "New approaches for axial magnetic bearings," in *The 7th International Symposium on Magnetic Bearings*, pp. 443–448, August 2000.

[11] N. Bianchi, S. Bolognani, and A. Cappello, "Reduction of cogging force in pm linear motors by pole-shifting," *IEE Proceedings Electric Power Applications*, vol. 152, pp. 703–709, May 2005.

[12] P. Hor, Z. Zhu, D. Howe, and J. Rees-Jones, "Minimization of cogging force in a linear permanent magnet motor," *IEEE Transactions on Magnetics*, vol. 34, pp. 3544 – 3547, September 1998.

[13] J.-K. Seok and T.-S. Hwang, "Cogging force reduction of two-phase linear hybrid stepping motor," *IEEE Transactions on Magnetics*, vol. 6, pp. 2202 – 2204, June 2005.

[14] J. Wang, M. Inoue, Y. Amara, and D. Howe, "Cogging-force-reduction techniques for linear permanent-magnet machines," *IEE Proceedings Electric Power Applications*, vol. 152, pp. 731 – 738, May 2005.

[15] M. Herrmann and H. Ulbrich, "Augmented control strategies and controller optimisation for compact actuators," in *Actuator 2006*, June 2006.